

Dynamic modeling and simulation of the multi-effect distillation desalination process

Jianqing Hu^a, Lianying Wu^{a,*}, Yan Wang^b, Weitao Zhang^a, Yangdong Hu^a

^aCollege of Chemistry and Chemical Engineering, Ocean University of China, Qingdao, Shandong, China, 266100, Tel. +8613791914873; emails: wulianying@ouc.edu.cn (L.Y. Wu), hujianqing.cool@163.com (J.Q. Hu), 55768616@qq.com (W.T. Zhang), ydhuhd@ouc.edu.cn (Y.D. Hu)

^bCollege of Chemistry and Chemical Engineering, Qingdao University, Qingdao, Shandong, China, 266071, email: yanwang@qdu.edu.cn

Received 22 May 2020; Accepted 20 November 2020

ABSTRACT

Accurate description and analysis of the dynamic behavior of state variables in multi-effect distillation (MED) desalination process is a challenge for its characteristic of numerous variables and their complex correlation. This paper is aimed at exploring the dynamic response of state variables with the derived dynamic model in MED desalination process, including evaporate temperature, salinity, evaporation mass flow rate and brine pool level. Adopting the reported modeling strategy, a rigorous dynamic model of the MED is established by coupling the dynamic equations of mass, salt and energy balance of the system, considering the relation between the state variables and the operating time. The dynamic model is solved in finite time and the influence on state variables is investigated under specific conditions, that is, by importing disturbance in feed temperature, feed flow and/or steam flow. From the point view of process control, the indices of maximum deviation (MD), response time (RT) and transition time (TT) are applied to analyze the transition process of state variables, serious parameters of which are significant for PID controller and control scheme deployment, especially in multistage and integrated process. The parameters of a designed nine effects advection MED plant in China are taken as the initial input data of the model in simulation and analysis part. Simulation results demonstrate the transition process and the approximate data of MD/RT/TT for the state variables in the case plant. The evaluation process might promote the practical application of dynamic simulation result for control scheme implement and the further control strategy research.

Keywords: Seawater desalination; Process modeling; Multi-effect distillation; Dynamic simulation

1. Introduction

With the global issue of water shortage to be solved urgently, seawater desalination, as an open source throttling technology to the worldwide challenge has aroused widespread attention. A variety of desalination technologies have been developed on the basis of thermal distillation or membrane separation technique during the last several decades, such as multi-stage flash (MSF), multiple-effect distillation (MED), vapor compression distillation, reverse

osmosis (RO), membrane distillation crystallization, etc. [1–7]. It is viewed that three processes namely MSF, MED and RO have been the dominant technologies for the high performance ratio (PR) of fresh water [8,9]. Comparing with membrane separation process, MED/MSF takes the advantage of simple material and energy flow. MED and MSF are usually driven by low-grade source with lower equipment investment as well [10]. Moreover, the power consumption of an MED plant is significantly lower than that of an MSF

* Corresponding author.

plant. MED is more efficient than MSF from a thermodynamic and heat transfer point of view [11,12]. As reported in the literature [13], some plants have been built to operate with a top brine temperature in the first effect of about 70°C, which reduces the energy consumption and the potential of seawater scaling. Recent development in thermally activated desalination methods has achieved an energy efficiency less than 2.5 (kW h_{elec})/m³ [14]. Furthermore, with the synthesis technology of different desalination processes and heat transfer enhancement technology developing, hybrid desalination process based on MED will play a more important role in the future [15,16].

In order to improve the PR and decrease the energy consumption of fresh water, current MED is designed with approximately 10 stages with heat transfer temperature difference between 2°C and 5°C [17]. As a result of the tiny temperature difference in adjacent stages, operating conditions should be controlled within a small margin of error to guarantee the MED desalination system in stable production state. Otherwise, the MED desalination system might run off the designed parameters, leading to severe issues such as local overheating, severe scaling and decline of production [18,19]. On the other hand, various integrated desalination process has been proposed [20,21], the control system design of which is an important step for industrial practice. Precise control scheme and unit should be designed seriously to deal with the random external disturbances manually or environmentally. The large-scale process control of highly complex desalination plants has been largely occupied with conventional proportional-integral-derivative (PID) controllers [22]. Although conventional techniques may provide a minimum performance requirement, they fall short of the increasing control performance demand of stability as the stage number increases. Control systems in desalination plants are responsible for keeping the parameters of the plant within the specified allowable design limits. Therefore, the first step for control scheme designers is to observe the behavior of state variables in the system, once the disturbance is imposed. Shahzad et al. [23] had carried out an experiment on MEDAD hybrid desalination cycle and extracted the typical temperature profiles for the start-up of the three-stage MED plant, which provided a great contribution for further application of the hybrid process. However, it might be unrealistic for most of the plant to build the experimental device to get the state variable profiles. Dynamic modeling and simulation would be a preferred choice.

Obviously, accurate simulation model is vital for the purpose of grasp the transition process distinctly. To date, a large variety of modeling works have been performed for the simulation of steady-state operations of the MED process. It is impossible to design an accurate and efficient process control system for MED desalination process with steady-state model. The dynamic model, which is particularly important in improving both the stability and the operational efficiency of the plant, can be employed to predict behaviors of the plant under transient conditions. El-Nashar and Qamhiyeh [24] developed a dynamic model on MED systems for predicting the transient behavior of multi-effect stack-type (MES) distillation plants. This model was validated by comparing the calculated data with actual

plant operation data obtained from MES evaporator at Abu Dhabi solar desalination plant, while both results exhibit reasonable agreement. Calle et al. [25] reported a dynamic model for simulating a pilot MED plant located at CIEMAT-Plataforma Solar de Almería (PSA) using a compound solar collector, in which the solar energy was employed as heat source. Narmine [26] established a dynamic model of the multi-effect evaporation, who investigated the variation of state variables in the evaporator when the heating steam flow reduces by 10%. Nevertheless, the fluctuation of other input variables was not discussed. Later, another dynamic model based on mass and energy balance equations for the PF-MED-TVC system was proposed by Narmine's group. In this model, a modified Runge-Kutta method was applied to solve the differential equations simultaneously. In another case, Mazini et al. [27] developed a dynamic model for MED-TVC plants depending on mass and energy balances of brine and water. The brine salinity, brine level and temperature were selected as state variables to describe the dynamics of each effect. However, the variation of the TVC motive steam flow rate was not analyzed. Shahzad and Ng [28] presented a transient model for the hybrid MED plus adsorption/desorption (AD) system and compared with conventional MED systems. Azimibavil and Dehkordi [29] reported a method for the predication of the MED unit dynamics, in which the dynamic behaviors of both water and vapor streams in the tube bundle of an effect were emphasized. Simulation results are of importance for the control of wall fouling in heat transfer tubes. Nevertheless, this work merely focused on analyzing a single effect, while the information on the behavior of an entire MED plant was missing. Ge et al. [30] presented a start-up model of MED in combination with a nuclear heating reactor. In this model, both the evaporators and the preheaters in each effect were expressed through mass and energy conservations. However, the model formulation is more likely to describe the sequence of stationary conditions of a system, rather than the representation of a real dynamic model for the MED process. Roca et al. [31] developed a dynamic model for the solar-assisted MED pilot unit. The aim of this dynamic model is to implement a control process for optimizing the distillate production. The proposed model gives key indications toward improving the thermal performance of MED under transient operating conditions.

As mentioned above, various dynamic simulation models have been proposed and validated. What is important to the proposed work is the dynamic model for MED with thermal vapor compressor plant from Mazini et al. [27], which adopting the modeling strategy that the evaporator unit is divided into three main subsystems; evaporators (effects), condenser and thermo-compressor, considering the evaporate temperature, salinity, and the brine pool level as the state variables. Thus the inner characteristic could be observed, especially the transition process once the disturbance imposed. As far as the process control engineer concerned, the process transition identification is of significance for PID controller design and control scheme deployment [32]. For instance, the fluctuant deviation and discrete time are employed to evaluate the effectiveness of the designed control systems [33]. In accordance with the general process of control system design [34],

maximum deviation (MD), response time (RT) and transition time (TT) are adopted to analyze the process identification in this paper.

This paper is organized as follows: in Section 2, process description of MED is given and mathematical dynamic model of the plant is derived based on the mass, salt and heat balance equations as well as numerous physical property equations. The evaporate temperature, salinity, and the brine pool level could be observed when solving the derived model. In sections 3, dynamic simulations of single-effect evaporator state variables are carried out by MATLAB software for analyzing the dynamic characteristics of the process. In section 4, the dynamic change behavior of state variables for MED process is investigated by applying disturbance of input variables including the feed water temperature, the seawater flow or the steam flow, and how the dynamic simulation results could be used for control scheme design. Finally, section 5 provides some concluding remarks.

2. Dynamic model

2.1. Description of the evaporation process

According to the heat and mass transfer process, a single evaporator can be divided into three lumps, that is, the brine pool, vapor space and tube bundle. Graphical representation of a single effect including three lumps is shown in Fig. 1.

As illustrated in Fig. 2, the pre-effective steam is piped through the heating tube bundle while the feed water is uniformly sprayed from the top of the evaporator on the outer wall of the heat transfer tube bundle. The steam turns into water entering the water chamber. Part of the feed water vaporizes into the steam chamber. Meanwhile, the liquid part is mixed with the salt water from the last effect in the brine pool.

2.2. Dynamic model of the MED

Dynamic simulation of the MED process is aimed at observing the regularity of the state variables in practical engineering. Therefore, the consistency of the dynamic

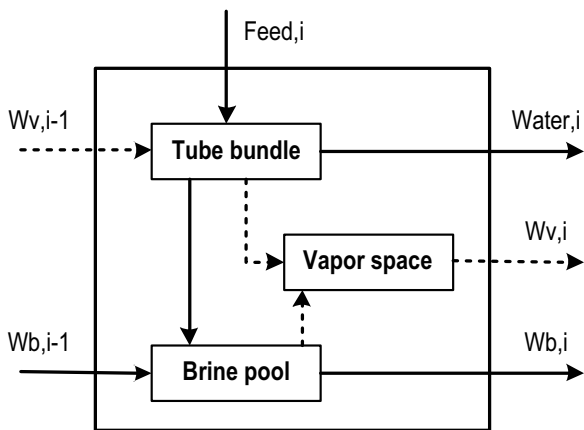


Fig. 1. Internal structure of the evaporator.

model is considered to be a key factor. Adopting the modeling strategy from literature [27], the differential dynamic model can be deduced based on mass, heat, salt balance and seawater physical property equations. The derivation process is presented, as follows:

BPE correlation:

$$T_{b,i} = T_{v,i} + BPE_i \quad (1)$$

with differentiation from Eq. (1):

$$\frac{dT_{b,i}}{dt} = \frac{dT_{v,i}}{dt} + \frac{dBPE_i}{dt} \quad (2)$$

BPE is the function of steam temperature and salinity

$$\frac{dT_{b,i}}{dt} = \left[1 + \frac{\partial BPE_i}{\partial T_i} \right] \frac{dT_{v,i}}{dt} + \frac{dBPE_i}{dX_i} \frac{dX_i}{dt} \quad (3)$$

The quality and density correlation:

$$M_{b,i} = A_s \times L_i \times \rho_i \quad (4)$$

with differentiation from Eq. (4):

$$\frac{dM_{b,i}}{dt} = A_s \times \rho_i \times \frac{dL_i}{dt} + A_s \times L_i \times \left(\frac{\partial \rho_i}{\partial T_{b,i}} \frac{\partial T_{b,i}}{\partial t} + \frac{\partial \rho_i}{\partial X_i} \frac{\partial X_i}{\partial t} \right) \quad (5)$$

The flow rate of evaporation:

$$W_{v,i} = \frac{W_{v,i-1}L_{i-1} - W_{\text{feed}}C_{\text{pf}}(T_i - T_{\text{feed}}) + W_{b,i-1}C_{\text{pb}}(T_{i-1} - T_i)}{L_i} \quad (6)$$

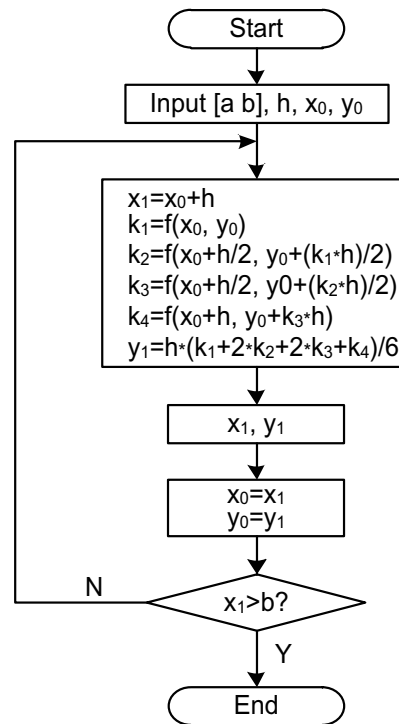


Fig. 2. Flow chart of the Runge-Kutta method.

The derivation of mass balance equation:

$$\frac{dM_{b,i}}{dt} = W_F + W_{b,i-1} - W_{b,i} - W_{v,i} \quad (7)$$

Combining Eqs. (3), (5)–(7), the following equation is obtained for the mass balance equations:

$$k_1 \frac{dL_i}{dt} + k_2 \frac{dT_i}{dt} + k_3 \frac{dX_i}{dt} = k_4 \quad (8)$$

where

$$\begin{cases} k_1 = A_s \times \rho_i \\ k_2 = A_s \times \frac{\partial \rho_i}{\partial T_{b,i}} \left(1 + \frac{\partial \text{BPE}_i}{\partial T_i} \right) \\ k_3 = A_s \times L_i \times \left(\frac{\partial \rho_i}{\partial T_{b,i}} \frac{\partial \text{BPE}_i}{\partial X_i} + \frac{\partial \rho_i}{\partial X_i} \right) \\ k_4 = W_F + W_{b,i-1} - W_{b,i} - W_{v,i} \end{cases}$$

The derivation of energy balance equation:

$$\frac{d(M_{b,i} \times h_{b,i})}{dt} = W_F \times h_F + W_{b,i-1} \times h_{b,i-1} - W_{b,i} \times h_{b,i} - W_{v,i} \times h_{v,i} + Q_{E,i} \quad (10)$$

where

$$Q_{E,i} = Wv_{i-1} \times hv_{i-1} = K_i \times A_{s,i} \times \text{LMTD} \quad (11)$$

$$\text{LMTD} = \frac{(T_{v,i-1} + T_{\text{feed}}) - 2T_{v,i}}{\ln \left(\frac{T_{v,i-1} - T_{v,i}}{T_{v,i} - T_{\text{feed}}} \right)} \quad (12)$$

Combining Eqs. (3), (5)–(7) and (10), the following equation is obtained for the energy balance equations:

$$k_5 \frac{dL_i}{dt} + k_6 \frac{dT_i}{dt} + k_7 \frac{dX_i}{dt} = k_8 \quad (13)$$

where

$$\begin{cases} k_5 = A_s \times h_{b,i} \times \rho_i \\ k_6 = A_s \times L_i \times \rho_i \times \frac{\partial h_{b,i}}{\partial T_{b,i}} \left(1 + \frac{\partial \text{BPE}_i}{\partial T_i} \right) + A_s \times L_i \times h_{b,i} \times \frac{\partial \rho_i}{\partial T_{b,i}} \left(1 + \frac{\partial \text{BPE}_i}{\partial T_i} \right) \\ k_7 = A_s \times L_i \times \rho_i \times \left(\frac{\partial h_{b,i}}{\partial T_{b,i}} \frac{\partial \text{BPE}_i}{\partial X_i} + \frac{\partial h_{b,i}}{\partial X_i} \right) + A_s \times L_i \times h_{b,i} \times \left(\frac{\partial \rho_i}{\partial T_{b,i}} \frac{\partial \text{BPE}_i}{\partial X_i} + \frac{\partial \rho_i}{\partial X_i} \right) \\ k_8 = W_F h_F + W_{b,i-1} h_{b,i-1} - W_{b,i} h_{b,i} - W_{v,i} h_{v,i} + Q_{E,i} \end{cases} \quad (14)$$

The derivation of salt balance equation:

$$\frac{d(M_{b,i} \times X_{b,i})}{dt} = W_F \times X_F + W_{b,i-1} \times X_{b,i-1} - W_{b,i} \times X_{b,i} \quad (15)$$

Combining Eqs. (3), (5)–(7) and (15), the following equation is obtained for the salt balance equations:

$$k_9 \frac{dL_i}{dt} + k_{10} \frac{dT_i}{dt} + k_{11} \frac{dX_i}{dt} = k_{12} \quad (16)$$

where

$$\begin{cases} k_9 = A_s \times \rho_i \times X_i \\ k_{10} = A_s \times X_i \times \frac{\partial \rho_i}{\partial T_{b,i}} \left(1 + \frac{\partial \text{BPE}_i}{\partial T_i} \right) \\ k_{11} = A_s \times L_i \times \left(X_i \times \frac{\partial \rho_i}{\partial T_{b,i}} \frac{\partial \text{BPE}_i}{\partial X_i} + X_i \times \frac{\partial \rho_i}{\partial X_i} + \rho_i \right) \\ k_{12} = W_F X_F + W_{b,i-1} X_{b,i-1} - W_{b,i} X_i \end{cases} \quad (17)$$

Thus, we can write derivatives of three mentioned state variables using Eqs. (8), (14) and (17) as follows:

$$\begin{cases} \frac{dL_i}{dt} = \frac{C \cdot E - B \cdot F}{A \cdot E - B \cdot D} \\ \frac{dT_i}{dt} = \frac{A \cdot F - C \cdot D}{A \cdot E - B \cdot D} \\ \frac{dX_i}{dt} = \frac{k_{12} - k_9 \frac{dL_i}{dt} - k_{10} \frac{dT_i}{dt}}{k_{11}} \end{cases} \quad (18)$$

where

$$\begin{cases} A = k_1 k_{11} - k_3 k_9 \\ B = k_2 k_{11} - k_3 k_{10} \\ C = k_4 k_{11} - k_3 k_{12} \\ D = k_5 k_{11} - k_7 k_9 \\ E = k_6 k_{11} - k_7 k_{10} \\ F = k_8 k_{11} - k_7 k_{12} \end{cases} \quad (19)$$

Eqs. (18) and (19) are the derived dynamic model of MED. So far, a few points about the model should be expounded in details. (i) The model is mainly based on Mazini's work, and model validation has been proved to be consistent with a real plant. (ii) The thermal vapor compressor model part is not included, for the proposed work is aimed to investigate the inner state variables of a nine-effect desalination during transition process. (iii) For simplification of the computational complexity, the heat transfer coefficient of steam condensation on each stage is

assumed to be a constant ($1,500 \text{ W m}^{-2} \text{ C}^{-1}$), which is recommended in chemical process equipment [35] and validated with experiment in literature [36].

Dynamic simulation is the numerical solution of the model at different time points, which is implemented via MATLAB software. The Runge–Kutta method (Fig. 2) is adopted for the numerical solution of the differential equations. Interval (h) is set as 1 s.

3. Dynamic analysis of the single-effect evaporator

3.1. Initial conditions

For transient simulations, the initialization of all time-differential variables depends on a number of initial conditions. Thus, fixed initial conditions (based on the data available from steady-state simulation results) are listed in Table 1. The data were extracted from a design case in desalination engineering [37]. It is important to note that all initial conditions (Table 1) are only used for the numerical initialization of the solver, but they cannot describe a specific initial status of the plant.

The dynamic simulation of the evaporation process is based on the determination of the structure and parameters of the equipment. The plant size of the evaporator is calculated according to the formula in the chemical process design manual and fundamentals of salt water desalination [38,39] based on initial conditions. Size of the plant is shown in Table 2.

Dynamic response of the single-effect evaporator to step disturbances is presented in the following sections.

3.2. Evaluation indices for transition process

The evaluation indices for transition process are presented in Fig. 3. MD is the maximum deviation between the initial and fluctuated value of state variables. RT is the delayed time of state variables when disturbance imposed. TT is the transition time of the whole process. The proposed work is aimed to simulate the multi-effect desalination (MED) plants in dynamic mode with disturbance of manipulated variables imposing and evaluating the transition process reasonably for control scheme research.

3.3. Dynamic characteristic analysis of the evaporator

The dynamic simulation time is 2 h. When step change of the sea water temperature is given at $t = 0.3 \text{ h}$, the variations of effect variables including evaporation temperature, brine level, brine concentration and evaporation rate in the evaporator is shown in Fig. 4.

As presented in Fig. 4, the first point that should be emphasized is that the state variables are in oscillation all the time as the dynamic model is solved with numerical methods (zoomed in Fig. 4). When the temperature of seawater rises by 5% at 0.3 h, the evaporation temperature increases from 69.1°C to 71°C. The maximum deviation is 2°C and the transition time is approximately 0.7 h. The evaporation rate increases from 9,480 to 10,000 kg/h and the transition time is approximately 0.7 h. The brine concentration increases and the transition

time is approximately 0.7 h. The brine pool level decreases with a maximum deviation of around 20% m. The settling time is about 1.1 h. These results of single-effect evaporator should be considered as the minimum boundary of MED system. Moreover, in order to perform the validation of the adopted model, the simulation result analysis of the proposed and published work [27] is shown in Table 3.

Table 1
Initial conditions of the dynamic simulation

Variable	Value
Feed (kg/h)	16,666
Sea water temperature (°C)	25
Seawater salinity (mass fraction)	0.035
Steam flow (kg/h)	10,000
Steam temperature (°C)	110
Heat transfer area (m ²)	476
Evaporation temperature (°C)	69.1
Salt chamber level (m)	0.5
Brine salinity (mass fraction)	0.068

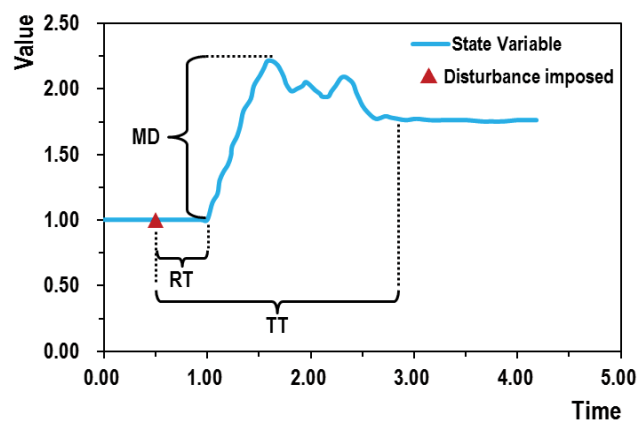


Fig. 3. Description of MD/RT/TT.

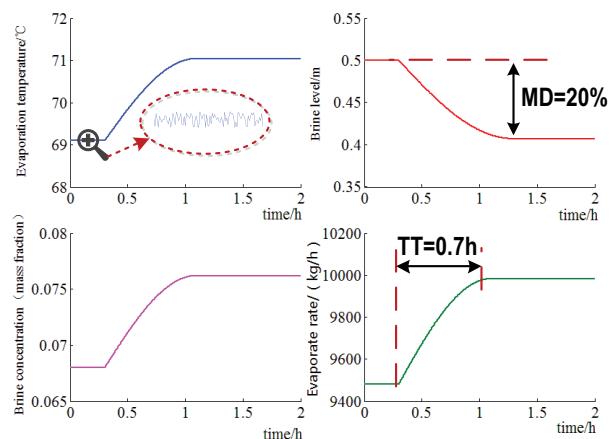


Fig. 4. Step response of the evaporator.

The temperature of each effect restores stable after the imposed disturbance (5% increase of feed water temperature). Temperature increase ratio is calculated from the initial and stable temperature both in simulation result and literature data. It should be noted that the temperature increase ratio is lower than that in the literature data, especially for the first effect. As the thermal compressor part belonging to the process intensification (PI) technique is not involved in the proposed work, it is reasonable that the temperature increase ratio is lower. Approximately, the simulation result is consistent with that in the literature and the model is validated.

4. Dynamic simulation and analysis of MED

To evaluate the system behavior under transient conditions, a series of analysis were carried out through simulating

Table 2
Size of the plant

Evaporator device size	
Diameter (m)	1
Tube bundle height (m)	1
Brine pool height (m)	1

Table 3
Analysis of the simulation result and literature data

ith effect	Simulation result			Literature data			Error magnitude
	Initial temperature (°C)	Stable temperature (°C)	Temperature increase ratio	Initial temperature (°C)	Stable temperature (°C)	Temperature increase ratio	
1	38.0	40.8	7.37%	46.4	57.2	23.28%	15.91%
2	40.5	42.7	5.43%	53.6	60.8	13.43%	8.00%
3	44.3	46.5	4.97%	57.0	62.1	8.95%	3.98%
4	48.2	50.2	4.15%	59.8	63.2	5.69%	1.54%
5	52.3	53.8	2.87%	62.1	64.8	4.35%	1.48%
6	56.5	57.0	0.88%	64.0	65.5	2.34%	1.46%

Table 4
Initial conditions of MED dynamic simulation

	1	1–2	2–3	3–4	4–5	5–6	6–7	7–8	8–9
ΔT (°C)	/	4.8	4.4	4.3	4.2	4.1	3.9	3.8	2.5
T_v (°C)	70	65.2	60.8	56.5	52.3	48.2	44.3	40.5	38
W_v (kg/h)	10,742	9,887	9,461	8,889	8,704	8,628	8,693	8,883	8,862
W_b (kg/h)	12,291	28,788	35,994	43,771	51,733	59,771	67,744	75,527	83,331
X (mass fraction)	0.073	0.071	0.069	0.068	0.068	0.068	0.069	0.070	0.070
Heat transfer area (m ²)	476	915	956	919	921	935	991	1,039	1,575
L (m)					0.5				
T_s (°C)					110				
F_s (kg/h)					13,784				
T_{sw} (°C)					25				
F_{sw} (kg/h)					166,666				
X_{sw}					0.035				

the presence of external disturbances with independent operating variables. In this study, effects of (i) seawater temperature, (ii) seawater flow rate and (iii) steam flow rate variation were investigated.

4.1. Initial conditions of MED

The initial conditions extracted from a designed case [38] for dynamic simulation are shown in Table 4. The dynamic behavior of state variables (temperature T , brine level L and brine concentration X) are observed by applying disturbance of feed water temperature, feed seawater flow or steam flow.

4.2. Effect of variation in feed water temperature

The effect of temperature variation in the inlet seawater is of great importance for the design of control systems and plant operation. As a matter of fact, feed water temperature can be easily manipulated by changing the operation of heat exchangers. Feed water is usually applied for cooling down the outlet streams of distillate or brine, and the feed water is pre-heating at the same time.

The step change of the feed water temperature is increased by 5% at 0.3 h. The dynamic response of the parameters (temperature, brine concentration, evaporation rate and brine level) in the process is shown in Fig. 5.

As shown in Fig. 5, when the feed water temperature increases, the evaporation temperature, the evaporation rate and the brine concentration increase, while the brine pool level drops. The MD from the first effect to the last effect increases gradually and the MD of brine level in last stage is 30%. The variables of each effect are responded simultaneously. The TT of each effect is different and the TT of the final effect is approximately 2.2 h.

4.3. Effect of variation in feed water flow rate

A similar analysis was performed to investigate the response of the system with increasing 5% of the feed seawater flow rate at 0.3 h. The behaviors of evaporation temperature, salinity (brine concentration), evaporation mass

flow rate and brine pool levels were observed, as reported in Fig. 6.

From Fig. 6, the liquid level of the brine chamber increases with increasing the feed water flow, whereas the evaporation and the salinity of brine decrease. The MD reduced gradually from the first effect to the end effect. The TT of each evaporator in turn increases along the brine flow direction, and the transition time of the final effect reaches the maximum value at 3.1 h.

4.4. Effect of variation in steam flow rate

Variation in the steam flow rate is key controlling operation in MED plants. Meanwhile, the influence of steam flow rate is significant for all variables, since it can

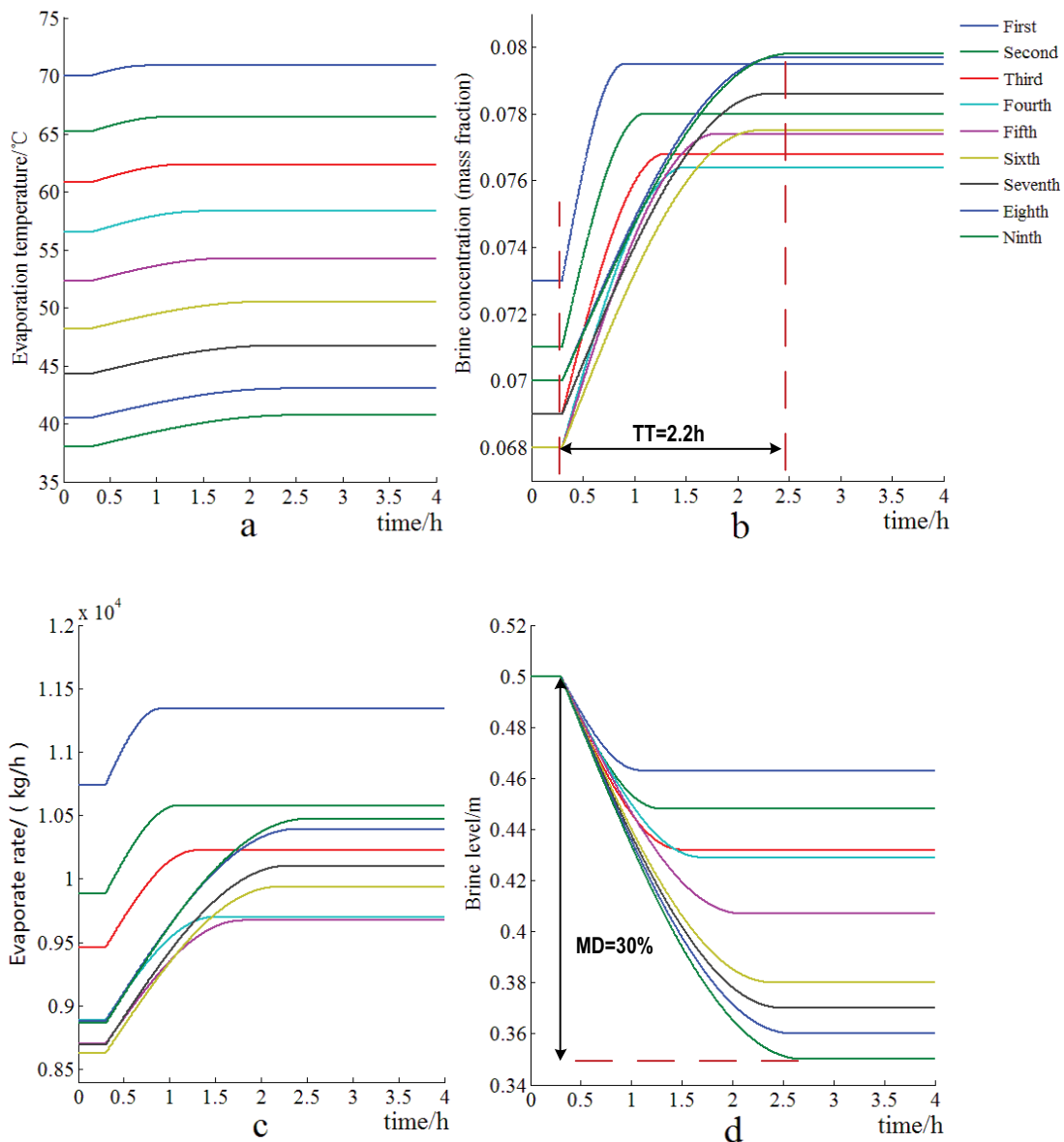


Fig. 5. Transient response of the system to a step variation of the feed water temperature: (a) evaporation temperature, (b) brine concentration, (c) evaporation rate, and (d) brine pool level.

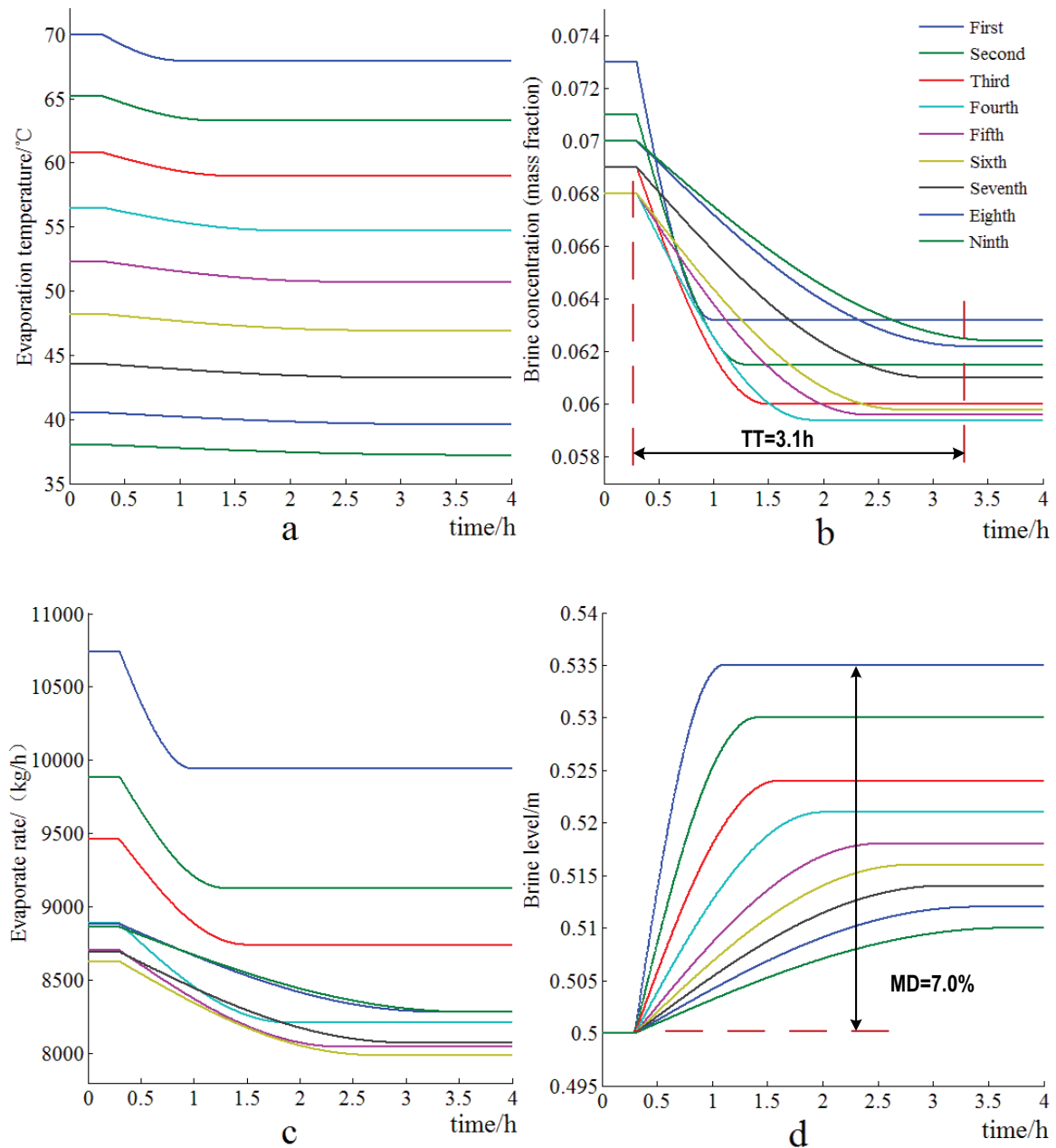


Fig. 6. Transient response of the system to a step variation of the feed water flow rate: (a) evaporation temperature, (b) brine concentration, (c) evaporate rate, and (d) brine pool level.

dramatically affect the distillate production rate and the gain output ratio of the unit.

The dynamic response of the system was analyzed for several operation variables with the steam flow rate increasing by 5% at 0.3 h, as shown in Fig. 7.

As shown in Fig. 7, when the steam flow rate increases, the evaporation temperature, the evaporation and the salinity increase, while the salt chamber level drops. The MD from the first effect to the end effect increases gradually. All effects are responded at the different times. The TT of each evaporator increases effect by effect and the transition time of the final effect achieves the maximum value at 3.5 h.

4.5. Simulation result analysis

The dynamic simulation has been performed in the front part. The evaporate temperature, brine concentration, evaporate rate and brine level are selected as the observed variables, the stability of which are vital in terms of fresh water productivity, energy consumption, safety operation or evaporator scaling. No doubt that all variables in the dynamic model could be observed for different need in control scheme design process. In this paper, the mentioned four variables are involved in the dynamic simulation part and the transition process of the variables is summarized in Table 5.

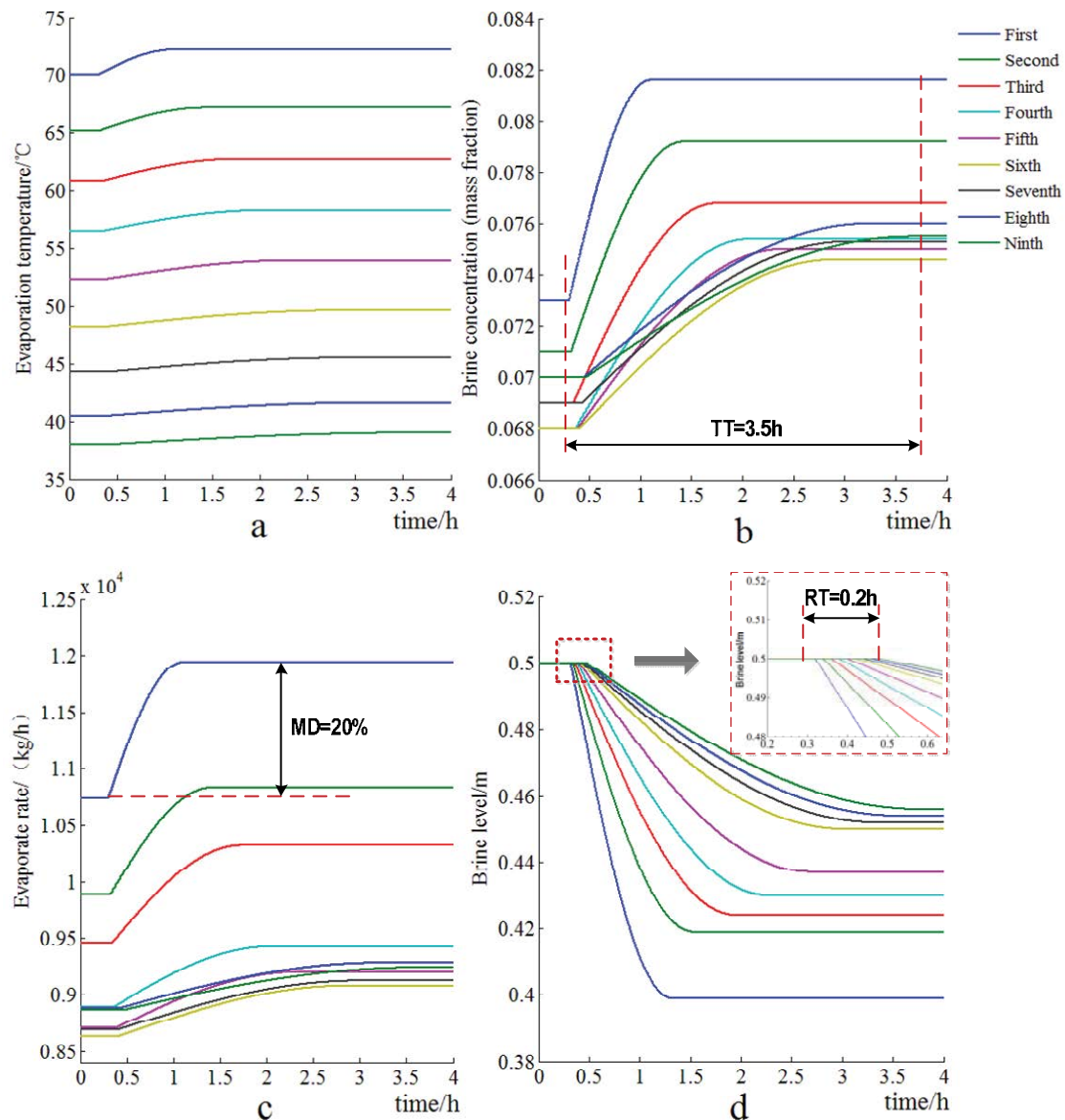


Fig. 7. Transient response of the system to a step variation of the feed steam rate: (a) Evaporation temperature, (b) brine concentration, (c) evaporation rate, and (d) brine pool level.

Table 5 has shown the evaluation of the transition process when different disturbance imposed. The maximum value has been marked out. It should be explained in details that the maximum value means to the whole MED system but not to one evaporator/unit, which is usually larger than that of one evaporator/unit. It is important to notice that amplification effect is one essential characteristics of multi process. Energy consumption saving and PR are benefitted from the amplification effect. However, the difficulty of keeping the system stable increases at the same time due to the amplification effect of deviation in cascade process. Control scheme designers should not only consider the evaporators transition process but also the MED system from top to end. The obtained result could be referred for further research of control scheme.

5. Conclusion

In this paper, a dynamic mathematical model based on mass, salt and energy conservations for the analysis of MED desalination plants was proposed. The Runge–Kutta method was adopted to solve the proposed model via MATLAB software. The steady-state simulation results were used as initial conditions to carry out a series of dynamic simulations. The maximum deviation (MD), RT and transition time (TT) are adopted to evaluate the dynamic behavior of the state variables (temperature T , liquid level L and salinity X) in the transition process. It is found that when the temperature of the feed water rises, the evaporation capacity, the evaporating temperature and the salinity of salt stream increase, whereas the liquid level drops. Maximum deviations of the evaporation amount,

Table 5
Evaluation of the transition process

Disturbance	Nine effect desalination state variables	Evaluation indices		
		MD/%	RT/h	TT/h
+5% Feed water temperature	Evaporate temperature	–	✓(0.0)	–
	Brine concentration	–	✓(0.0)	✓(2.2)
	Evaporate rate	–	✓(0.0)	–
	Brine level	✓(–30)	✓(0.0)	–
+5% Feed water flow rate	Evaporate temperature	–	✓(0.0)	–
	Brine concentration	–	✓(0.0)	✓(3.1)
	Evaporate rate	–	✓(0.0)	–
	Brine level	✓(+7.0)	✓(0.0)	–
+5% Steam flow rate	Evaporate temperature	✓(+20)	✓(0.2)	–
	Brine concentration	–	✓(0.2)	✓(3.5)
	Evaporate rate	–	✓(0.2)	–
	Brine level	–	✓(0.2)	–

the liquid level, the evaporator temperature and the brine salinity in the multi-effect evaporation system increase with the fluctuation of the steam flow rate and/or the feed seawater temperature, while they reduce with the fluctuation of the feed flow rate. When the feed flow rate and the feed temperature fluctuate, the state variables of each effect respond simultaneously. However, the state variables respond sequentially when the steam flow fluctuates. The simulation results are evaluated with the indices of MD/RT/TT, demonstrating the inner transition process of MED system. The dynamic simulation results provide a basis for the design of MED desalination process control system.

Symbols

i	–	i th effect of the MED process
L	–	Salt chamber level, m
X	–	Brine salinity, mass fraction
T, T_v	–	Vapor temperature, °C
T_b	–	Brine temperature/°C
h_v	–	Enthalpy of steam, kJ/kg
ρ	–	Brine density, kg/m ³
BPE	–	Boiling point elevation, °C
M_b	–	Brine flow, kg/h
A_s	–	Heat transfer area, m ²
W_F	–	Feed water flow, kg/h
X_F	–	Seawater salinity, mass fraction
T_s	–	Steam temperature, °C
T_{sw}	–	Sea water temperature, °C
X_{sw}	–	Sea water brine salinity, mass fraction
t	–	Time, h
T_{feed}	–	Sea water temperature, °C
W_b	–	Brine flow, kg/h
W_v	–	Evaporation flow, kg/h
h_F	–	Enthalpy of seawater, kJ/kg
h_b	–	Enthalpy of brine, kJ/kg
C_{pf}	–	Specific heat capacity of water, kJ/(kg °C)
C_{pb}	–	Specific heat capacity of brine, kJ/(kg °C)
LMTD	–	Logarithmic mean temperature difference, °C

K	–	Heat transfer coefficient, W/(m K)
Δt	–	Designed temperature difference, °C
Q_E	–	Heat transfer rate of evaporator, kW
F_s	–	Steam flow rate, kg/h
F_{sw}	–	Sea water flow rate, kg/h

Acknowledgment

The authors are grateful to the financial support from the National Nature Science Fund Program of China (No. 21376231 and No. 21776264).

References

- [1] M. Shatat, S.B. Riffat, Water desalination technologies utilizing conventional and renewable energy sources, *Int. J. Low-Carbon Technol.*, 9 (2014) 1–19.
- [2] F. Salata, M. Coppi, A first approach study on the desalination of sea water using heat transformers powered by solar ponds, *Appl. Energy*, 136 (2014) 611–618.
- [3] M.W. Shahzad, M. Burhan, N. Ghaffour, K.C. Ng, A multi evaporator desalination system operated with thermocline energy for future sustainability, *Desalination*, 435 (2018) 268–277.
- [4] M.W. Shahzad, K.C. Ng, An improved multievacaporator adsorption desalination cycle for gulf cooperation council countries, *Energy Technol.*, 5 (2017) 1663–1669.
- [5] M.W. Shahzad, K.C. Ng, On the road to water sustainability in the Gulf, *Nat. Middle East*, 50 (2016), doi: 10.1038/nmiddleeast.2016.50.
- [6] Y.-D. Kim, K. Thu, A. Myat, K.C. Ng, Numerical simulation of solar-assisted multi-effect distillation (SMED) desalination systems, *Desal. Water Treat.*, 51 (2013) 1242–1253.
- [7] H.T. Wang, B.A. Li, B. Liu, Status of seawater desalination technology and presents of novel technology, *Sal. Chem. Ind.*, 6 (2014) 1–5.
- [8] M.W. Shahzad, M. Burhan, K.C. Ng, A standard primary energy approach for comparing desalination processes, *NPJ Clean Water*, 1 (2019) 1–7.
- [9] K.C. Ng, M.W. Shahzad, H.S. Son, O.A. Hamed, An exergy approach to efficiency evaluation of desalination, *Appl. Phys. Lett.*, 110 (2017) 1841011–1841015, <https://doi.org/10.1063/1.4982628>.

- [10] M.W. Shahzad, K.C. Ng, K. Thu, Future sustainable desalination using waste heat: kudos to thermodynamic synergy, *Environ. Sci. Water Res. Technol.*, 2 (2016) 206–212.
- [11] A.D. Khawaji, I.K. Kutubkhanah, J.-M. Wie, Advances in seawater desalination technologies, *Desalination*, 221 (2008) 47–69.
- [12] M.A. Darwish, *Desalination Process: A Technical Comparison*, Proceedings of IDA World Congress on Desalination and Water Sciences, Abu Dhabi, United Arab Emirates, 1995, pp. 149–173.
- [13] A. Ophir, A. Gendel, G. Kronenberg, The LT-MED process for SW Cogen plants, *Desal. Water Reuse.*, 4 (1994) 28–31.
- [14] M.W. Shahzad, K. Thu, K.C. Ng, W.G. Chun, Recent development in thermally activated desalination methods: achieving an energy efficiency less than $2.5 \text{ kWh}_{\text{elec}}/\text{m}^3$, *Desal. Water Treat.*, 57 (2016) 7396–7405.
- [15] M.W. Shahzad, K.C. Ng, K. Thu, B.B. Saha, W.G. Chun, Multi effect desalination and adsorption desalination (MEDAD): a hybrid desalination method, *Appl. Therm. Eng.*, 2 (2014) 289–297.
- [16] K.C. Ng, K. Thu, S.J. Oh, L. Ang, M.W. Shahzad, A.B. Ismail, Recent developments in thermally-driven seawater desalination: energy efficiency improvement by hybridization of the MED and AD cycles, *Desalination*, 356 (2015) 255–270.
- [17] C.J. Gao, G.L. Ruan, *Seawater Desalination Technology and Engineering*, Chemical Industry Publications, Beijing, 2016 (in Chinese).
- [18] F.N. Alasfour, M.A. Darwish, A.O. Bin Amer, Thermal analysis of ME–TVC+MEE desalination systems, *Desalination*, 174 (2005) 39–61.
- [19] C.L. Li, X.Y. He, Study on Model-Free Adaptive Control in Multiple-Effect Evaporator Method, *J. Hunan Univ. Technol.*, 5 (2008) 74–76.
- [20] M.W. Shahzad, M. Burhan, K.C. Ng, Pushing desalination recovery to the maximum limit: membrane and thermal processes integration, *Desalination*, 416 (2017) 54–64.
- [21] T.M. Missimer, K.C. Ng, K. Thuw, M.W. Shahzad, Geothermal electricity generation and desalination: an integrated process design to conserve latent heat with operational improvements, *Desal. Water Treat.*, 57 (2016) 23110–23118.
- [22] S.W. Sung, J.T. Lee, I.-B. Lee, *Process Identification and PID Control*, Wiley-IEEE Press, 2009.
- [23] M.W. Shahzad, K. Thu, Y.-D. Kim, K.C. Ng, An experimental investigation on MEDAD hybrid desalination cycle, *Appl. Energy*, 148 (2015) 273–281.
- [24] A.M. El-Nashar, A. Qamhiyeh, Simulation of the performance of MES evaporators under unsteady state operating conditions, *Desalination*, 79 (1990) 65–83.
- [25] A. de la Calle, J. Bonilla, L. Roca, P. Palenzuela, Dynamic modeling and simulation of a solar-assisted multi-effect distillation plant, *Desalination*, 357 (2015) 65–76.
- [26] N.H. Aly, M.A. Marwan, Dynamic response of multi-effect evaporators, *Desalination*, 114 (1997) 189–196.
- [27] M.T. Mazini, A. Yazdizadeh, M.H. Ramezani, Dynamic modeling of multi-effect desalination with thermal vapor compressor plant, *Desalination*, 353 (2014) 98–108.
- [28] M.W. Shahzad, K.C. Ng, K. Thu, B.B. Saha, W.G. Chun, Multi-effect desalination and adsorption desalination (MEDAD): a hybrid desalination method, *Appl. Therm. Eng.*, 72 (2014) 289–297.
- [29] S. Azimibavil, A.J. Dehkordi, Dynamic simulation of a multi-effect distillation (MED) process, *Desalination*, 392 (2016) 91–101.
- [30] Z.H. Ge, X.Z. Du, L.J. Yang, Y.P. Yang, S.R. Wu, Simulation on the start-up of MED seawater desalination system coupled with nuclear heating reactor, *Appl. Therm. Eng.*, 28 (2008) 203–210.
- [31] L. Roca, L.J. Yebra, M. Berenguel, D.C. Alarcón-Padilla, Modeling of a solar seawater desalination plant for automatic operation purposes, *Sol. Energy Eng.*, 130 (2008) 1–8, <https://doi.org/10.1115/1.2969807>.
- [32] H. Chaudhary, V. Panwar, N. Sukavanum, R. Prasad, Fuzzy PD+I based hybrid force/position control of an Industrial Robot Manipulator, *IFAC Proc. Volumes*, 47 (2014) 429–436.
- [33] M.X. Lu, A. Luo, *Chemical Process Control System*, Chemical Industry Publications, Beijing, 2006 (in Chinese).
- [34] J. Carvajal, G.R. Chen, H. Ogmen, *Fuzzy PID Controller: Design, Performance Evaluation, and Stability Analysis*, Information Sciences, 2000.
- [35] J.R. Couper, W.R. Penney, J.R. Fair, *Chemical Process Equipment-Selection and Design*, Elsevier, Amsterdam, 2004.
- [36] M.W. Shahzad, A. Myat, W.G. Chun, K.C. Ng, Bubble-assisted film evaporation correlation for saline water at sub-atmospheric pressures in horizontal-tube evaporator, *Appl. Therm. Eng.*, 50 (2013) 670–676.
- [37] S.C. Wang, *Desalination Engineering*, Chemical Industry Publications, Beijing, 2006, pp. 39–46 (in Chinese).
- [38] D.R. Wu, *Chemical Process Design Handbook*, Chemical Industry Publications, Beijing, 2009, (in Chinese).
- [39] H.T. El-Dessouky, H.M. Ettouney, *Fundamentals of Salt Water Desalination*, Elsevier, Amsterdam, 2002.